

# Optimization of Lattice Boltzmann Simulations on Heterogeneous Computers

Journal Title  
XX(X):1–18  
©The Author(s) 0000  
Reprints and permission:  
sagepub.co.uk/journalsPermissions.nav  
DOI: 10.1177/ToBeAssigned  
www.sagepub.com/



E. Calore<sup>1</sup>, A. Gabbana<sup>1</sup>, S. F. Schifano<sup>1</sup>, R. Tripiccione<sup>1</sup>

## Abstract

High-performance computing systems are more and more often based on accelerators. Computing applications targeting those systems often follow a host-driven approach in which hosts offload almost all compute-intensive sections of the code onto accelerators; this approach only marginally exploits the computational resources available on the host CPUs, limiting performance and energy efficiency. The obvious step forward is to run compute-intensive kernels in a concurrent and balanced way on both hosts and accelerators. In this paper we consider exactly this problem for a class of applications based on Lattice Boltzmann Methods, widely used in computational fluid-dynamics. Our goal is to develop just one program, portable and able to run efficiently on several different combinations of hosts and accelerators. To reach this goal, we define common data layouts enabling the code to exploit efficiently the different parallel and vector options of the various accelerators, and matching the possibly different requirements of the compute-bound and memory-bound kernels of the application. We also define models and metrics that predict the best partitioning of workloads among host and accelerator, and the optimally achievable overall performance level. We test the performance of our codes and their scaling properties using as testbeds HPC clusters incorporating different accelerators: Intel Xeon-Phi many-core processors, NVIDIA GPUs and AMD GPUs.

## Keywords

Lattice Boltzmann methods, Accelerators, Performance modeling, Heterogeneous systems, Performance portability

## 1 Background and related works

The architecture of high-performance computing (HPC) systems is increasingly based on accelerators; typical HPC systems today – including several leading entries of the TOP500 list ([1]) – are large clusters of processing nodes interconnected by a fast low-latency network, each node containing standard processors coupled with one or more accelerator units.

Accelerators promise higher computing performance and better energy efficiency, improving on traditional processors up to one order of magnitude; in fact, they

- allow massive parallel processing by a combination of a large number of processing cores and vector units,
- allow for massive multi-threading, in order to hide

memory access latencies and, iii) trade a streamlined control structure (e.g., executing instructions in-order only) for additional data-path processing for a given device or energy budget.

Typical accelerated applications usually follow a host-driven approach in which the host processor offloads (almost) all compute-intensive sections of the code onto accelerators; the host itself typically

---

<sup>1</sup>University of Ferrara and INFN Ferrara, via Saragat 1, I-44122 Ferrara, ITALY.

### Corresponding author:

Sebastiano Fabio Schifano, University of Ferrara and INFN Ferrara, via Saragat 1, I-44122 Ferrara, ITALY.

Email: schifano@fe.infn.it

only orchestrates global program flow or processes sequential segments of the application; this approach wastes a non negligible amount of the available computational resources, reducing overall performance and energy efficiency.

The obvious step forward is that even compute-intensive application kernels should be executed in a balanced way on both hosts and accelerators. This improvement has been hampered so far by several non trivial obstacles, especially because CPUs and accelerators often present different architectures, so efficient accelerated codes may involve different data structures and operation schedules. Moreover, the lack of well established performance-portable programming heterogeneous frameworks has so far required the use of specific programming languages (or at least proprietary variants of standard languages) on each different accelerator, harming portability, maintainability and possibly even correctness of the application.

Improvements on this latter aspect come with the recent evolution of *directive*-based programming environments, allowing programmers to annotate their codes with hints to the compiler about available parallelization options. Several such frameworks have been proposed, such as the Hybrid Multi-core Parallel Programming model (HMPP) proposed by CAPS, hiCUDA ([2]), OpenMPC ([3]) and StarSs ([4]). However, the most common compiler frameworks currently used for scientific codes are OpenMP ([5]) and OpenACC ([6]). Both frameworks allow to annotate codes written in standard languages (e.g., C, C+ and Fortran) with appropriate *pragma* directives characterizing the available parallelization space of each code section. This approach leaves to compilers to apply all optimization steps specific to each different target architecture and consistent with the directives, allowing in principle portability of codes between any supported host and accelerator device. This process is still immature, and significant limits to portability still exist. The OpenMP standard, version 4 ([7]), has introduced support for – in principle – any kind of accelerator, but compilers supporting GPUs are not yet available, and the Intel Xeon Phi is de-facto the only

supported accelerator. On the other hand OpenACC supports several different GPUs and more recently also multi-core CPU architectures, but not the Xeon-Phi, and does not allow to compile codes able to spread parallel tasks concurrently on both GPU and CPU cores. Also, both standards do not address processor-specific hardware features so non-portable proprietary directives and instructions are often necessary; for example performance optimization on Intel CPU processors often requires Intel-proprietary compiler directives.

In spite of these weaknesses, and in the hope that a converging trend is in progress, one would like to i) understand how difficult it is to design one common code using common domain data structures running concurrently on host(s) and accelerator(s), that is portable and also performance-portable across traditional processors and different accelerators, and ii) quantify the performance gains made possible by concurrent execution on host and accelerator.

In order to explore this problem, one has to understand the impact on performance that different data layouts and execution schedules have for different accelerator architectures. One can then define a common data layout and write a common code for a given application with optimal (or close to optimal) performance on several combinations of host processors and accelerators. Assuming we can identify a common data layout giving good performance on several combinations of host processors and accelerators, then one has to find efficient partitioning criteria to split the execution of the code among hosts and processors.

In this paper we tackle exactly these issues for a class of applications based on Lattice Boltzmann (LB) methods, widely used in computational fluid-dynamics. This class of applications offers a large amount of easily identified available parallelism, making LB an ideal target for accelerator-based HPC systems. We consider alternate data layouts, processing schedules and optimal ways to compute concurrently on host and accelerator. We quantify the impact on performance, and use these findings to develop production-grade massively parallel codes. We run benchmarks and test

our codes on HPC systems whose nodes have dual Intel Xeon processors and a variety of different accelerators, namely the NVIDIA K80 ([8]) and AMD Hawaii GPUs ([9]), and the Intel Xeon-Phi ([10]).

Over the years, LB codes have been written and optimized for large clusters of commodity CPUs ([11]) and for application-specific machines ([12, 13, 14]). More recent work has focused on exploiting the parallelism of powerful traditional many-core processors ([15]), and of power-efficient accelerators such as GP-GPU ([16, 17, 18]) and Xeon-Phi processors ([19]), and even FPGAs ([20]).

Recent analyses of optimal data layouts for LB have been made in [21, 22, 23]. However, [21] focuses only on the *propagate* step, one of the two key kernels in LB codes, while [22] does not take into account vectorization; in [23] vectorization is considered using intrinsic functions only. None of these papers considers accelerators. In [24] we have started preliminary investigation considering only the Xeon-Phi as an accelerator. Here, we extend these results in several ways: first, we take into account both *propagate* and *collision* steps used in LB simulations. Then we use a high level approach based on compiler directives, and we take into account also NVIDIA and AMD accelerators commonly used in HPC communities. Very recently, [25, 26] have explored the benefits of LB solvers on heterogeneous systems considering different memory layouts and system based both on NVIDIA GPUs and Xeon-Phi accelerators. In our contribution we consider a more complex LB solver (D2Q37 instead of D2Q9) a wider analysis of data layouts and an automatic analytic way to find the optimal partitioning of lattice domains between host-CPU and accelerators.

This paper is structured as follows: section 2 introduces the main hardware features of CPUs and GPUs that we have taken into account in this paper and section 3 gives an overview of LB methods. Section 4 discusses the design and implementation options for data layouts suitable for LB codes and measures the impact of different choices in terms of performances, while section 5 describes the implementation of codes that we have developed concurrently running on both

host and accelerator. Section 6 describes two important optimization steps for our heterogeneous code and defines a performance model, while section 7 analyzes our performance results on two different clusters, one with K80 GPUs and one with Xeon-Phi accelerators. Finally, section 8 wraps up our main results and highlights our conclusions.

## 2 Architectures of HPC systems

Heterogeneous systems have recently enjoyed growing popularity in the HPC landscape. These systems combine within a single processing node commodity multi-core architectures with off-chip accelerators, GPUs, Xeon-Phi many-core units and (sometimes) FPGAs. This architectural choice comes from an attempt to boost overall performance adding an additional processor (the accelerator) that exploits massively parallel data-paths to increase performance (and energy efficiency) at the cost of reduced programming flexibility. In this section we briefly review the architectures of the state-of-the-art accelerators that we have considered – GPUs and Xeon-Phi many-core processors – focusing on the impact that their diverging architectures have on the possibility to develop a common HPC code able to run efficiently on both of them.

GPUs are multi-core processors with a large number of processing units, all executing in parallel. The NVIDIA K80 is a dual GK210 GPU, each containing 13 processing units, called streaming multiprocessors (SMX). Each processing unit has 192 compute units, called CUDA-cores, concurrently executing groups of 32 operations in a SIMT (Single Instruction, Multiple Thread) fashion; much like traditional SIMD processors, cores within a group execute the same instruction at the same time but are allowed to take different branches (at a performance penalty). The AMD FirePro W9100 is conceptually similar to the K80 NVIDIA GPU; it has 44 processing units, each one with 64 compute units (stream processors).

The clock of an NVIDIA K80 has a frequency of 573 MHz which can be boosted up to 875 MHz. The

	Xeon E5-2630 v3	Xeon-Phi 7120P	Tesla K80	FirePro W9100
#physical-cores	8	61	2 × 13 SMX	44
#logical-cores	16	244	2 × 2496	2816
Clock (GHz)	2.4	1.238	0.560	0.930
Peak perf. (DP/SP GF)	307/614	1208/2416	1870/5600	2620/5240
SIMD unit	AVX2 256-bit	AVX2 512-bit	N/A	N/A
L1 cache (MB)	20	30.5	1.68	1.00
#Mem. Channels	4	16	–	–
Max Memory (GB)	768	16	2 × 12	16
Mem BW (GB/s)	59	352	2 × 240	320

**Table 1.** Selected hardware features of the systems tested in this work: Xeon E5-2630 is a commodity processor adopting the Intel Haswell micro-architecture; Xeon-Phi 7120P is based on the Intel MIC architecture; Tesla K80 is a NVIDIA GPU with two Tesla GK210 accelerators; FirePro W9100 is an AMD Hawaii GPU

aggregate peak performance is then of 5.6 TFlops in single precision and 1.87 TFlops in double precision (only one third of the SMXs work concurrently when performing double precision operations). Working at 930MHz the processing units of the AMD FirePro W9100 delivers up to 5.2 TFlops in SP and 2.6 in DP.

In general, GPUs sustain their huge potential performance thanks to large memory bandwidth – in order to avoid starving the processors – and massive multi-threading – to hide memory access latency. Consequently, register files are huge in GPUs, as they have to store the states of many different threads, while data caches are less important. For example (see also Table 1), a K80 GPU has a combined peak memory bandwidth of 480 GB/s, while each SMX has a register file of 512KB and just 128KB L1 cache/shared memory; SMX units share a 1536KB L2 cache. Similarly, the AMD W9100 has a peak memory bandwidth of 320 GB/s and its last level cache is just 1MB.

The architecture of Xeon-Phi processors – the other class of accelerators that we consider – builds on a very large number of more traditional X86 cores, each optimized for streaming parallel processing, with a streamlined and less versatile control part and enhanced vector processing facilities. For instance, the currently available version of this processor family – the Knights Corner (KNC) – integrates up to 61 CPU cores, each supporting the execution of 4 threads, for an aggregate peak performance of 1 TFlops in double precision, with a clock running at 1.2 GHz. Each core has a 32 KB L1-cache and a 512 KB L2-cache. The

L2-caches, private at the core level, are interconnected through a bi-directional ring and data is kept coherent and indirectly accessible by all cores. The ring also connects to a GDDR5 memory bank of 16 GB, with a peak bandwidth of 352 GB/s. Each core has a Vector Processing Unit (VPU), executing SIMD operations on vectors of 512 bits.

Present generation GPUs and Xeon-Phi processors are connected to their host through a PCI-express interface, allowing data exchange between the two processors. Typically 16 PCI-express lanes are used, with an aggregate bandwidth of 8 GB/s, much smaller than the typical memory bandwidth of these processors, so processor-accelerator data exchanges may easily become serious performance bottlenecks.

For both processor classes, in this work we consider a host-driven heterogeneous programming model, with applications executing both on the host and on the accelerator \*. So far, different programming languages have been available for each specific accelerator; indeed, NVIDIA GPUs have a proprietary programming language, and AMD GPUs are supported by the OpenCL programming environment. On the contrary, the Xeon-Phi uses the same programming environment as its Xeon multi-core counterpart, so one can develop codes following a directive-based approach (e.g. OpenMP), slightly reducing the effort of application migration. On the other hand, many works have shown that extracting a large fraction of the performance capabilities of the Knights Corner (KNC), the first generation Xeon Phi co-processors, still requires significant efforts and fine restructuring of the code.

Following recent improvements in directive-based programming environments, the present work wants to explore ways of writing common codes that i) have optimization features that can be exploited by

---

\*the Xeon-Phi also support “native mode” thus acting as an independent node capable of running applications independently. This approach will be enhanced in the next generation Xeon-Phi system, the Knights Landing, that will also be available as a stand alone processor. We do not consider this mode of operation in this paper.

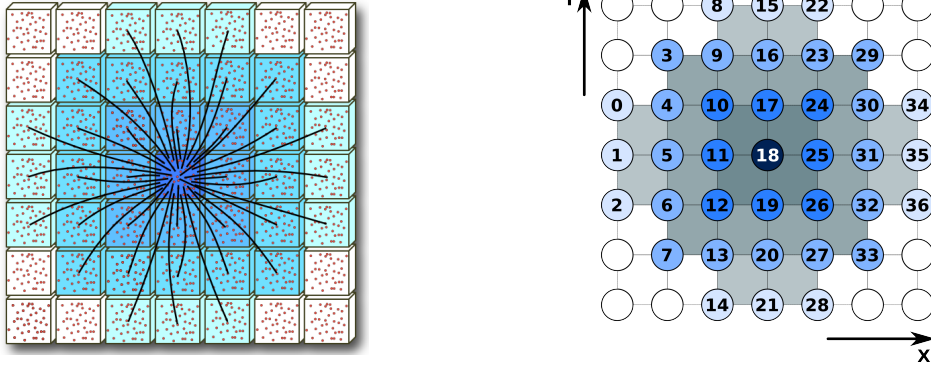


**Figure 1.** Left: Velocity vectors for the LB populations of the D2Q37 model. Right: populations are identified by an arbitrary label, associated to the lattice hop that they perform in the *propagate* phase.

traditional CPUs and both accelerator architectures, and ii) are written using a common directive-based (e.g. OpenMP, OpenACC) programming environment.

### 3 Lattice Boltzmann methods

In this section, we sketchily introduce the computational method that we adopt, based on an advanced Lattice Boltzmann (LB) scheme. LB methods (see [27] for an introduction) are discrete in position and momentum spaces; they are based on the synthetic dynamics of *populations* sitting at the sites of a discrete lattice. At each time step, populations hops from lattice-site to lattice-site and then they *collide*, mixing and changing their values accordingly.

Over the years, several LB models have been developed, describing flows in 2 or 3 dimensions, and using sets of populations of different size (a model in  $x$  dimensions based on  $y$  populations is labeled as  $DxQy$ ). Populations ( $f_i(x, t)$ ), each having a given lattice velocity  $\mathbf{c}_i$ , are defined at the sites of a discrete and regular grid; they evolve in (discrete) time according to the Bhatnagar-Gross-Krook (BGK) equation:

$$f_i(\mathbf{x} + \mathbf{c}_i \Delta t, t + \Delta t) = f_i(\mathbf{x}, t) - \frac{\Delta t}{\tau} \left( f_i(\mathbf{x}, t) - f_i^{(eq)} \right) \quad (1)$$

The macroscopic physics variables, density  $\rho$ , velocity  $\mathbf{u}$  and temperature  $T$  are defined in terms of the  $f_i(x, t)$

and  $\mathbf{c}_i$  variables:

$$\rho = \sum_l f_l \quad \rho \mathbf{u} = \sum_l \mathbf{c}_l f_l \quad D\rho T = \sum_l |\mathbf{c}_l - \mathbf{u}|^2 f_l;$$

the equilibrium distributions ( $f_l^{(eq)}$ ) are themselves functions of these macroscopic quantities ([27]). With an appropriate choice of the set of lattice velocities  $\mathbf{c}_i$  and of the equilibrium distributions  $f_l^{(eq)}$ , one shows that, performing an expansion in  $\Delta t$  and re-normalizing the values of the physical velocity and temperature fields, the evolution of the macroscopic variables obeys the thermo-hydrodynamical equations of motion and the continuity equation:

$$\begin{aligned} \partial_t \rho + \rho \partial_i u_i &= 0, \\ \rho D_t u_i &= -\partial_i p - \rho g \delta_{i,2} + \nu \partial_{jj} u_i, \\ \rho c_v D_t T + p \partial_i u_i &= k \partial_{ii} T; \end{aligned} \quad (2)$$

$D_t = \partial_t + u_j \partial_j$  is the material derivative and we neglect viscous heating;  $c_v$  is the specific heat at constant volume for an ideal gas,  $p = \rho T$ , and  $\nu$  and  $k$  are the transport coefficients;  $g$  is the acceleration of gravity, acting in the vertical direction. Summation of repeated indexes is implied.

In our case we study a 2-dimensional system ( $D = 2$  in the following), and the set of populations has 37 elements (hence the D2Q37 acronym) corresponding to (pseudo-)particles moving up to three lattice points away, as shown in Figure 1 ([28, 29]). The main advantage of this recently developed LB method is

that it automatically enforces the equation of state of a perfect gas ( $p = \rho T$ ). Our optimization efforts have made it possible to perform large scale simulations of convective turbulence in several physics conditions (see e.g., [30, 31]);

An LB code starts with an initial assignment of the populations, corresponding to a given initial condition at  $t = 0$  on some spatial domain, and iterates Equation 1 for each population and lattice site and for as many time steps as needed; boundary conditions are enforced at the edges of the domain after each time step by appropriately modifying population values at and close to the boundary.

From the computational point of view, the LB approach offers a huge degree of easily identified available parallelism. Defining  $\mathbf{y} = \mathbf{x} + \mathbf{c}_l \Delta t$  and rewriting the main evolution equation as:

$$f_l(\mathbf{y}, t + \Delta t) = f_l(\mathbf{y} - \mathbf{c}_l \Delta t, t) - \frac{\Delta t}{\tau} \left( f_l(\mathbf{y} - \mathbf{c}_l \Delta t, t) - f_l^{(eq)} \right) \quad (3)$$

one easily identifies the overall structure of the computation that evolves the system by one time step  $\Delta t$ : for each point  $\mathbf{y}$  in the discrete grid the code: i) gathers from neighboring sites the values of the fields  $f_l$  corresponding to populations drifting towards  $\mathbf{y}$  with velocity  $\mathbf{c}_l$  and then, ii) performs all mathematical steps needed to compute the quantities in the r.h.s. of Equation 3. One quickly sees that there is no correlation between different lattice points, so both steps can proceed in parallel on all grid points according to any convenient schedule, with the only constraint that step 1 precedes step 2.

As already remarked, our D2Q37 model correctly and consistently describes the thermo-hydrodynamical equations of motion and the equation of state of a perfect gas; the price to pay is that, from a computational point of view, its implementation is more complex than for simpler LB models. This translates in demanding requirements for memory bandwidth and floating-point throughput. Indeed, step 1 implies accessing 37 neighbor cells to gather all

populations, while step 2 implies  $\approx 7000$  double-precision floating point operations per lattice point, some of which can be optimized away e.g. by the compiler.

## 4 Data-layout optimization for LB kernels

Our goal is to design a performance-portable code capable of running efficiently on recent Intel multi-core CPUs as well as on Xeon-Phi and GPU accelerators.

Our intendedly common application is written in plain C and annotated with compiler directives for parallelization. For Intel architectures, we have used OpenMP and proprietary Intel directives, using the offload pragmas to run kernels on the Xeon-Phi. For NVIDIA and AMD GPUs we have annotated the code with OpenACC directives, implemented by the PGI compiler, which supports both architectures. Mapping OpenACC directives on OpenMP directives is almost straightforward, so code divergence is limited at this point in time; it is expected that OpenMP implementations supporting both classes of accelerators will become available in the near future, so we hope to be able soon to merge the two versions into one truly common code.

As remarked in section 1, data layout has a critical role in extracting performance from accelerators.

Data layouts for LB methods, as for many other stencil applications, have been traditionally based either on *array of structures* (AoS) or on *structure of arrays* (SoA) schemes. Figure 2 shows how population data are stored in the two cases; in the AoS layout, population data for each lattice site are stored one after the other at neighboring memory locations. This scheme exhibits locality of populations at a given lattice site, while populations of common index  $i$  at different lattice sites are stored in memory at non unit-stride addresses. Conversely, in the SoA scheme for a given index  $i$ , populations of all lattice sites are stored contiguously, while the various populations of each lattice site are stored far from each other at non unit-stride addresses.

```

#define N (LX*LY)
typedef struct {
  data_t p1; // population 1
  data_t p2; // population 2
  ...
  data_t p37; // population 37
} pop_t;

pop_t lattice[N];

```

```

#define N (LX*LY)
typedef struct {
  data_t p1[N]; // population 1
  data_t p2[N]; // population 2
  ...
  data_t p37[N]; // population 37
} pop_t;

pop_t lattice;

```

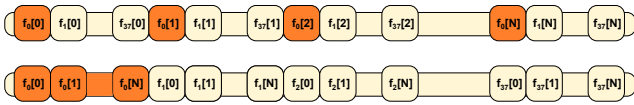


**Figure 2.** Top and Middle: C definitions of lattice populations using the AoS and SoA data layouts. Bottom: Graphic representation of the AoS and SoA layout.

In our implementation we have arbitrarily chosen to store the lattice in column-major order ( $Y$  spatial direction); we keep in memory two copies that are alternatively read and written by each kernel routine. Although demanding in terms of memory requirements, this choice has the key advantage that it allows in principle to process all lattice sites in parallel.

#### 4.1 Data-layout optimization for propagate

In our LB code the `propagate` kernel is applied to each lattice site, moving populations according to the patterns of Figure 1. For each site, `propagate` reads and writes populations from lattice cells at distance up to 3 in the physical lattice and for this reason locality of memory accesses plays an important role for performance.

This kernel can be implemented using either a *push* or a *pull* scheme, [21]. The former moves all populations of a lattice site towards appropriate neighboring sites, while the latter gathers to one site populations stored at neighbor sites. Relative advantages and disadvantages of these schemes are not obvious and depend to some extent on the hardware

features of the target processor. While the *push* scheme performs an aligned-read followed by a misaligned-write, the opposite happens if the *pull* scheme is used, and it is well known that reading/writing from/to (non-)aligned memory addresses may have a large impact on the sustained memory bandwidth of modern processors, [32]. However, on cache-based Intel architectures (both standard CPUs and Xeon-Phi), aligned data can be stored directly to memory using *non-temporal* write instructions. If data to be stored is not resident at any cache level, standard semantic of ordinary memory-writes require a prior read for ownership (RFO); the *non-temporal* version of store avoids the RFO read, improving effective memory bandwidth and saving time. This feature can be used in the *pull* scheme reducing the overall memory traffic by a factor 1/3, so we adopt it.

The `propagate` kernel can in principle be vectorized applying each move shown in Figure 1 to several lattice sites in parallel, e.g. moving populations with the same index  $i$  and belonging to two or more sites. The number of sites processed in parallel depends on the size of the vector instructions of the target processor; vector size is 4 double words for the Xeon-CPU, 8 for the Xeon-Phi, 32 or multiples thereof for GPUs. However, using the AoS scheme, populations of different sites are stored at non-contiguous memory addresses preventing vectorization. Conversely, when using the SoA layout, access to several populations of index  $i$  has unit stride, allowing to move in parallel populations of index  $i$  for several sites and allowing vectorization. This discussion suggests that the SoA layout should perform better than the AoS one. Figure 3 (left) shows the C-code written for Intel processors, adopting the SoA layout. The code sweeps all lattice sites with two loops in the  $X$  and  $Y$  spatial directions. The inner loop is on  $Y$ , as elements are stored in column-major order. We have annotated this loop with the `#pragma omp simd` OpenMP pragma to introduce SIMD vector instructions. Since values of populations written into `nxt` array are not re-used within this kernel, we also enable *non-temporal* stores; since this feature is not yet part of the OpenMP

```

typedef data_t double;
typedef struct { data_t s[LX*LY]; } pop_soa_t;

pop_soa_t prv[NPOP], nxt[NPOP];

#pragma omp parallel for
for ( ix = STARTX; ix < ENDX; ix++ ) {
  #pragma vector nontemporal
  for ( iy = STARTY; iy < ENDY; iy++ ) {
    idx = IDX(ix, iy);
    for ( ip = 0; ip < NPOP; ip++ ) {
      nxt[ip].s[idx] = prv[ip].s[ idx + OFF[ip] ];
    }
  }
}

```

```

typedef data_t double;
typedef struct { data_t s[LX*LY]; } pop_soa_t;

pop_soa_t prv[NPOP], nxt[NPOP];

#pragma acc kernels present(prv, nxt)
#pragma acc loop gang independent
for ( ix = STARTX; ix < ENDX; ix++ ) {
  #pragma acc loop vector independent
  for ( iy = STARTY; iy < ENDY; iy++ ) {
    idx = IDX(ix, iy);
    for ( ip = 0; ip < NPOP; ip++ ) {
      nxt[ip].s[idx] = prv[ip].s[ idx + OFF[ip] ];
    }
  }
}

```

**Figure 3.** Codes of the propagate kernel for Intel architectures (left) and GPUs (right). This kernel moves populations as shown in Figure 1. OFF is a vector containing the memory address offsets associated to each population hop. The prv and nxt arrays use the SoA layout.

Data Structure	Haswell	Xeon Phi	Tesla K80	AMD Hawaii
propagate				
AoS	408	194	326	649
SoA	847	224	36	57
CSoA	247	78	32	45
CAoSoA	286	89	33	50
collide				
AoS	1232	631	767	2270
SoA	1612	1777	171	1018
CSoA	955	445	165	452
CAoSoA	812	325	166	402

**Table 2.** Execution time (milliseconds per iteration) of the propagate and collide kernels on several architectures using different data-layouts. The size of the lattice is  $2160 \times 8192$  points.

standard we have used the specific Intel directive `#pragma vector nontemporal`. The equivalent code for GPUs, replacing Intel and OpenMP directives with corresponding OpenACC ones, is shown in Figure 3 (right).

The first two rows of Table 2 compare the performance obtained with the two layouts on all the processors that we consider. As expected the SoA layout is much more efficient on GPUs, but this is not true for both Intel processors; inspection of the assembly codes and compiler logs shows that read operations are not vectorized on Intel processors due to *unaligned* load addresses. Lacking vectorization, the AoS layout exhibits a better performance as it has a better cache hit rate.

The reason why compilers fail to vectorize the code is that load addresses are computed as the sum of the destination-site address – which is memory-aligned – and an offset, so they point to the neighbor sites from which populations are read. This does not guarantee that the resulting address is properly aligned to the vector size, i.e. 32 Bytes for CPUs and 64 Bytes for the Xeon-Phi. Store addresses on the other hand are always aligned if the lattice base address is properly aligned and  $Y$  is a multiple of 32 or 64.

A simple modification to the data layout solves this problem. Starting from the lattice stored in the SoA scheme, we cluster VL consecutive elements of each population array, with VL a multiple of the hardware vector size supported by the processor (e.g. 4 for the Haswell CPU, 8 for the Xeon-Phi and 32 for GPUs). We call this scheme *Cluster Structure of Array* (CSoA); in Figure 4 we show the corresponding C type definitions, `vdata_t` and `vpop_soa_t`. `vdata_t` holds VL data words corresponding to the same population of index  $i$  at VL different sites that can be processed in SIMD fashion. `vpop_soa_t` is the type definition for the full lattice data. Using this scheme, move operations generated by propagate apply to clusters of populations and not to individual population elements. Since clusters have the same size as hardware vectors, all read operations are now properly aligned. As in the case of the SoA data layout, write operations always have aligned accesses and non temporal stores can be used. Figure 4 shows



```

#define LYOVL (LY / VL)
typedef data_t double;
typedef struct { data_t c[VL]; } vdata_t;

typedef struct { vdata_t s[LX*LYOVL]; } vpop_soa_t;

vpop_soa_t prv[NPOP], nxt[NPOP];

for ( ix = startX; ix < endX; ix++ ) {
    idx = ix*LYOVL;
    for( ip = 0; ip < NPOP; ip++ ) {
        for ( iy = startY; iy < endY; iy++ ) {
            #pragma vector aligned nontemporal
            for(k = 0; k < VL; k++) {
                nxt[ip].s[idx + iy].c[k] =
                    prv[ip].s[idx + iy + OFF[ip]].c[k];
            }
        }
    }
}

```

**Figure 4.** Source code of the propagate kernel for Intel architectures using the CSoA data layout. OFF is a vector containing the memory-address offsets associated to each population hop. VL is the size of a cluster (see text for details). To properly vectorize the inner loop with SIMD instructions, value of VL should match the width of vector-registers supported by the target architecture.

the corresponding code; in this case we have also rearranged the order of the loops in a way which reduces the pressure on the TLB cache. As before, code for GPUs can be obtained replacing directives with *OpenAcc* ones.

Table 2 (see first three rows of the `propagate` section) quantifies the impact of the data layout on performance, showing benchmark results using the three different data layouts, AoS, SoA and CSoA. The advantages of using the CSoA data layout are large for Intel architectures, while improvements are marginal for GPUs, as they are less sensitive to misaligned memory reads [32]. The relevant result is however that using the CSoA format we have one common data layout that maximizes performance for `propagate` on all processors.

## 4.2 Data-layout optimization for collide

The `collide` kernel is computed after the `propagate` step, reading at each lattice site populations gathered by the `propagate` phase. It updates their values applying the *collisional* operator and performing all mathematical operations associated with Equation 1.

Metric	CSoA	CAoSoA	Threshold
Xeon-Phi			
L1 TLB Miss Ratio	2.66%	0.06%	1.0%
L2 TLB Miss Ratio	2.00%	0.00%	0.1%
Xeon-CPU			
LLC Miss Count	787,647,256	177,010,620	n/a
Average Latency (cycles)	13	9	n/a

**Table 3.** Profiling results provided by the Intel VTune profiler for the `collide` kernel on a lattice of  $2160 \times 8192$  points comparing the CSoA and the CAoSoA scheme on the Xeon-CPU and Xeon-Phi processors.

For each lattice site, this floating point intensive kernel uses only population data associated to the site on which it operates; lattice sites are processed independently from each other making processing of the lattice fully parallelizable. In this case, in contrast with the `propagate` kernel, locality of populations plays an important role for performances. Vectorization of this step is implemented, as for `propagate`, trying to process different sites in parallel.

Following results obtained in section 4.1 we consider first the CSoA data layout which – as seen before – gives very good performance results with the `propagate` kernel. The log files of the compiler show that the CSoA scheme allows to vectorize the code, but profiling the execution of the code on Xeon CPUs and Xeon Phi accelerators, we have observed a large number of TLB and LLC misses, suggesting that further improvements could be put in place. Table 3 shows the results (see CSoA column) provided by Intel VTune profiler for both Xeon-CPU and Xeon-Phi; for the latter the miss ratios are much bigger than threshold values provided by the profiler itself. These penalties arise because in the CSoA scheme different populations associated to the same lattice site are stored at memory addresses far from each other, so several non-unit stride memory accesses are necessary to gather all relevant data words.

To overcome these problems, we further modify the CSoA scheme, and define a new data layout which takes into account locality requirements of both `propagate` and `collide` kernels. In this scheme, for each population array, we divide each *Y*-column in VL partitions each of size LY/VL; all elements sitting at the

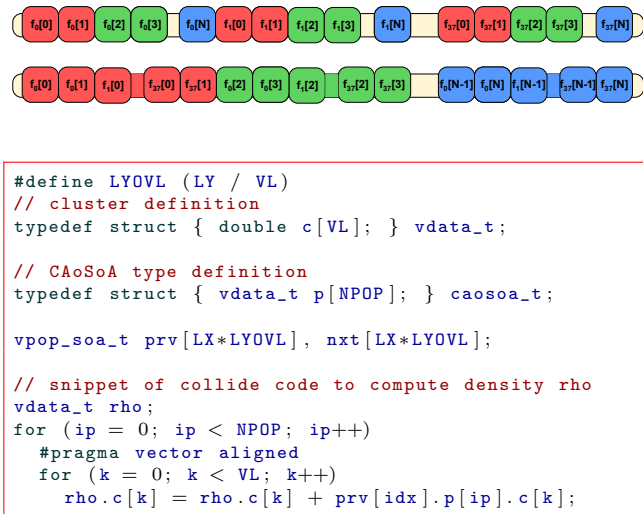


**Figure 5.** Top: data arrangement for the CAoSoA layout; for illustration purposes, we take  $VL=2$ . Bottom: sample code for `collide` using this layout.

$i$ th position of each partition are then packet together into an array of  $VL$  elements called *cluster*. We call this layout a *Clustered Array of Structure of Array* (CAoSoA) and Figure 5 shows how data are arranged in memory. This data layout still allows vectorization of inner structures (clusters) of size  $VL$ , and at the same time improves locality – w.r.t the CSoA – of populations, as it keeps all population data needed to process each lattice site at close and aligned addresses. Figure 5 shows the definition of the `vdata_t` data type, corresponding to a *cluster*, and a representative small sections of the `collide` code for Intel processors. Cluster variables are processed iterating on all elements of the cluster through a loop over  $VL$ ; `pragma vector aligned` instructs the compiler to fully vectorize the loop since all iterations are independent and memory accesses are aligned. This data-layout combines the benefits of the CSoA scheme, allowing aligned memory accesses and vectorization (relevant for the *propagate* kernel) and at the same providing population locality (together relevant for the *collide* kernel).

Table 3 shows the impact of the CAoSoA data-layout on memory misses: on Xeon-Phi the TLB misses have been reduced well below the threshold values, and on Xeon-CPU have been reduced by a factor 4.5X w.r.t.

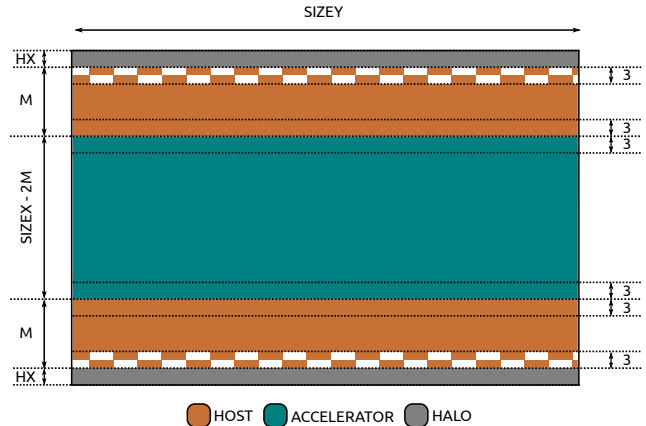


**Figure 6.** Logic partitioning of the lattice domain among host and accelerator. The central (dark-green) region is allocated on the accelerator, side (orange and gray) regions on the host. Checkerboard textures flag lattice regions involved in MPI communications with neighbor nodes.

the CSoA scheme. Table 2 shows the execution time of the `collide` kernel run using all data data-layouts defined so far. As we see, the CAoSoA improves performances over the CSoA on Intel and AMD processors while for NVIDIA GPU the two layouts give marginal differences in performance. These gains in the performance of `collide` come at a limited cost (12 – 16%) for *propagate* on all architectures except for the K80, so CAoSoA maximizes the combined performances of the two kernels.

## 5 Heterogeneous implementation

In this section we describe the implementation of our code designed to involve and exploit compute capabilities of both host and accelerators. We only consider the CAoSoA layout, as it grants the best overall performances on all processors and accelerators that we have studied.

Our implementation uses MPI libraries and each MPI-process manages one accelerator. The MPI-process runs on the host CPU; part of the lattice domain is processed on the host itself, and part is offloaded and processed by the accelerator. Using one MPI-process per accelerator makes it easy to extend the implementation to a cluster of accelerators installed either on the same or on different hosts.

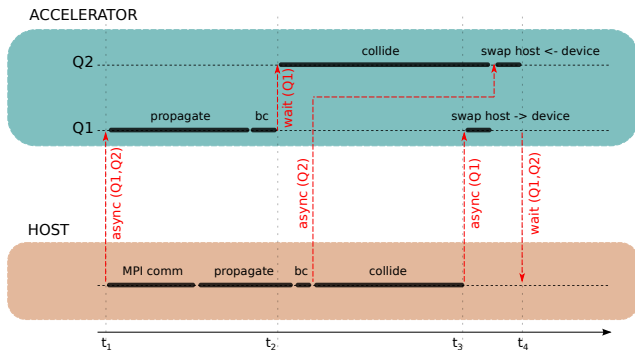


**Figure 7.** Control flow executed by each MPI-process. The schedule executed on the accelerator is on the upper band, while the one executed by the host is on the lower band. Execution on the accelerator runs on two concurrent queues. Synchronization-points are marked with red lines.

The lattice is partitioned among the MPI-processes, along one direction, in our case the  $X$ -direction, and each slice is assigned to a different MPI-process. Within each MPI-process each partition is further divided between host and accelerator. We define three regions, namely left border, bulk, and right border, as shown in Figure 6. The right and left borders include  $M$  columns and are allocated on the host memory while the remaining  $\text{SIZE}X - 2M$  columns stay on the accelerator memory. As `propagate` stencils require to access neighbor sites at distance up to 3, see Figure 1, each region is surrounded by a halo of three columns and rows. Each halo stores a copy of lattice sites of the adjacent region either allocated on the host, on the accelerator, or on the neighbor MPI-process. This arrangement allows to uniformly apply the `propagate` kernel to all sites avoiding divergences in the computation. An added advantage of this layout is that data involved in MPI communications is resident on the host and not on the accelerators, slightly increasing data locality.

Each MPI-process performs a loop over time steps, and at each iteration it launches in sequence on the accelerator the `propagate`, `bc` and `collide` kernels, processing the bulk region. In order to allow the CPU to operate in overlapped mode, kernels are launched asynchronously on the same logical execution queue to

ensure in-order execution. After launching the kernels on the accelerator, the host first updates halos with adjacent MPI-processes and then starts to process its left and right borders applying the same sequence of kernels. After the processing of borders completes, the host updates the halo regions shared with the accelerator; this step moves data between host and accelerator. The control-flow of the code executed by the MPI-process is shown in Figure 7, where the `bc` kernel applies the physical boundary conditions at the three uppermost and lowermost rows of the lattice.

The code for KNC is implemented using the offload features available in the Intel compiler and runtime framework. In this case we have a unique code and the compiler produces the executable codes for both Xeon-Phi and CPU. For GPUs the situation is somewhat different. In fact, we have to use two different compilers, one for GPUs and one for CPUs. We have written the code for GPUs, both NVIDIA and AMD, using *OpenACC* directives [33] and compiled using the PGI 16.5 compiler which supports both architectures. The kernels running on CPUs are written using standard C and compiled using Intel compiler ICC v16.0. Then we have linked the two codes in one single executable.

## 6 Parameter optimization

In this section we describe two important optimization steps for our heterogeneous code. The first is about the optimal partitioning of the computation between host and accelerator, and the latter is about the optimal cluster size for the CAoSoA data layout.

### 6.1 Workload partitioning

Hosts and accelerators have different peak (and sustained) performance, so a careful workload balancing between the two concurrent processors is necessary. We model the execution time  $T_{\text{exe}}$  of our code with the

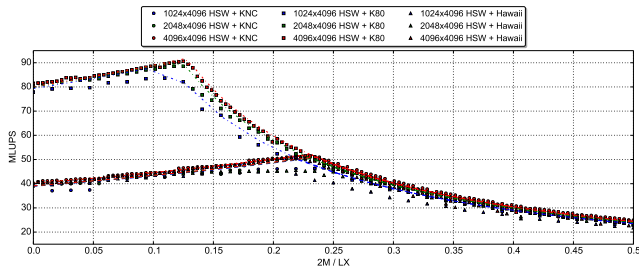


**Figure 8.** Performance of the heterogeneous code (measured in MLUPS, see the text for definition) for all three platforms, as a function of the fraction of lattice sites ( $2M/LX$ ) mapped on the Haswell (HSW) host CPU. KNC is the Intel Knights Corner accelerator, K80 is the NVIDIA Tesla GPU and Hawaii is the AMD GPU. Dots are measured values, dashed lines are the prediction of our model.

following set of equations:

$$T_{\text{exe}} = \max\{T_{\text{acc}}, T_{\text{host}} + T_{\text{mpi}}\} + T_{\text{swap}} \quad (4)$$

$$T_{\text{acc}} = (LX - 2M)LY \cdot \tau_d \quad (5)$$

$$T_{\text{host}} = (2M)LY \cdot \tau_h \quad (6)$$

$$T_{\text{mpi}} = \tau_c \quad (7)$$

where  $T_{\text{acc}}$  and  $T_{\text{host}}$  are the execution times of the accelerator and host respectively,  $T_{\text{swap}}$  is the time required to exchange data between host and accelerator at the end of each iteration, and  $T_{\text{mpi}}$  is the time to move data between two MPI-processes in a multi-accelerator implementation. As  $T_{\text{swap}}$  is independent of  $M$ ,  $T_{\text{exe}}$  is minimal for a value  $M^*$  for which the following equation holds:

$$T_{\text{acc}}(M^*) = T_{\text{host}}(M^*) + T_{\text{mpi}}(M^*) \quad (8)$$

Our code has an initial auto-tuning phase, in which it runs a set of mini-benchmarks to estimate approximate values for  $\tau_d, \tau_h, \tau_c$ . These are then inserted in Equation 8 to find  $M^*$ , an estimate of the value of  $M$  that minimizes time to solution.

In Figure 8 we show the performance of our code for three different lattice sizes as a function of  $2M/LX$ , the fraction of lattice sites that we map on the host CPU. We have run our tests on two different machines, the *Galileo* HPC system installed at *CINECA* and the *Etna* machine. *Galileo* has two different partitions,

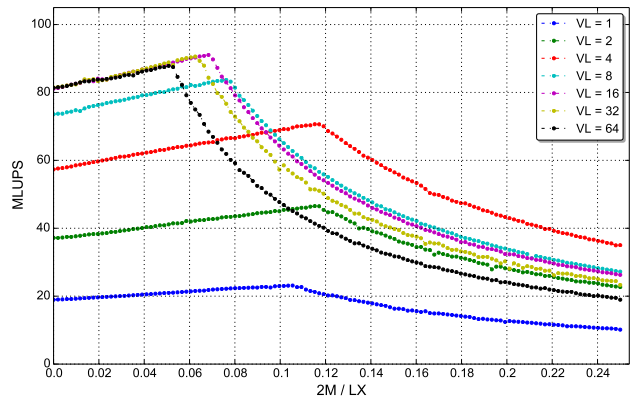


**Figure 9.** Performance (measured in MLUPS) for different values of the VL parameter in the CaoSoA data layout; results are for a Tesla K80 GPU.

one with K80 GPUs and one with KNC accelerators. The *Etna* machine is part of the *COKA* experimental cluster at *Università di Ferrara*, and has two AMD Hawaii GPUs. Both machines use as host processor an 8-core Intel Xeon E5-2630v3 CPU based on the *Haswell* micro-architecture, and each host has one attached accelerator. Performance is measured using the *MiLlion Updates per Second* (MLUPS) metric, a common option for this class of applications. In Figure 8 dots are measured values, while lines are our predictions. Our auto-tuning strategy predicts performance with good accuracy, and estimates the workload distribution between host and device for which the execution time reaches its minimum. An interesting feature of this plot is the fact that the optimal point is – for each accelerator – a function of  $2M/LX$ . As expected, for values of  $M < M^*$  and  $M > M^*$  performances decrease because the workload is unbalanced either on the accelerator or on the host side; results at  $2M/LX = 0$  correspond to earlier implementations in which critical kernels are fully offloaded to accelerators; we see that running these kernels concurrently on host and accelerators (KNC and K80) performances increases approximately by 10 – 20%. Finally, as  $M$  becomes much larger than  $M^*$ , all lines in the plot fall on top of each other, as in this limit the host CPU handles the largest part of the overall computation.

## 6.2 Fine-tuning of data-layout cluster size

An important parameter of the CAoS<sub>o</sub>A layout is the cluster size  $VL$ , as performance depends significantly on its value. This parameter, whose optimal value correlates with the hardware features of the target processor, affects data allocation in memory and must be fixed at compile time.

In Figure 9 we show the impact on performances (measured again in MLUPS) of our code running on a node with K80 GPUs and using different choices for  $VL$ . We see that, for this processor, a wrong choice may reduce performance by large factors ( $\simeq 5$ ); good news is that there is a reasonably large interval  $VL=16, 32, 64$  for which performance is close to its largest value. We have done the same measurements for all kind of nodes available with KNC and AMD GPUs, and then picked, for each node and each value of  $VL$ , the best operating point in terms of  $2M/LX$ . In this way, we select the highest performance for each combination of host and accelerator. These results are collected in Figure 10 as a function of  $VL$ ; on top of each bar we report the corresponding value of  $2M/LX$ . We see that GPUs are more robust than the KNC against a non optimal choice of  $VL$ : for the former processors performance remains stable as long as  $VL$  is large enough, while for the latter only one or two  $VL$  values allow to reach the highest performance. Fortunately enough, there is a window of  $VL$  values for which all systems are close to their best performance.

## 6.3 Performance prediction on new hardware

A further interesting result of the model developed in section 6.1, is that we can use it to predict to which extent the performance of our codes is affected if either the host CPU or the accelerator is replaced by a different processor; in particular one may ask what happens if announced but not yet available processors or accelerators are adopted. One such exercise replaces the host processor that we have used for our previous tests with the new Intel multicore Xeon E5-2697v4, based on the latest *Broadwell* micro-architecture. We have run our code

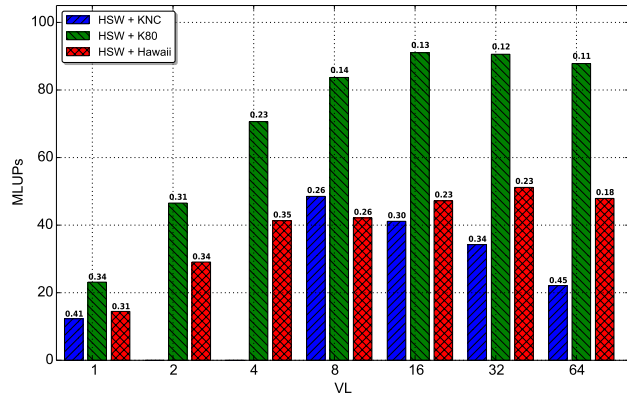


**Figure 10.** Impact on performance of different cluster sizes ( $VL$ ) in the CaoSoA data-layout for several accelerator choices.

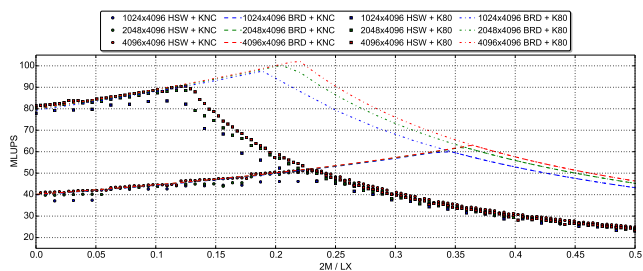


**Figure 11.** Performance predictions (dashed-lines) of our model for a would-be system using as host the recently-released Broadwell (BRD) CPU compared with measured data on a Haswell (HSW) CPU (dots). Measurements refer to three different lattice sizes.

on a *Broadwell* processor with no attached accelerators and measured the host-related performance parameters used in Equation 4; we have then used these parameters to estimate the expected performance of a would-be machine whose nodes combine Broadwell hosts with either K80 or KNC accelerators. Results are shown in Figure 11 where we compares the measured performance on the present hardware (dots) with the predictions of our model (dashed lines). We see that using this new more powerful processor, performance for our code would improve by approximately 20%, when perfectly balancing the workload between host and accelerator. As expected the improvement is the same for both types of accelerators, since we have only virtually replaced the host processor. Another interesting feature of the plot is that the model predictions overlap with measured data when  $2M/LX$

values tends to zero; this is expected, since in this case the fraction of lattice sites mapped on the host-CPU tends to zero and the execution time is dominated by the accelerator. A similar analysis might be performed, for instance, to assess the overall performance gains to be expected when next generation GPUs become available.

## 7 Scalability performances

In this section we analyze scalability performances of our codes running on the *Galileo* machine, both on the K80 and on the KNC partition.

In Figure 12 top-left we show the performance of our code running on larger and larger KNC partitions of the *Galileo* cluster, and for several physically relevant sizes of the physical lattice, showing the scaling results of this code. We compare with a previous v1 implementation of the code running all kernels on the KNC accelerator. Figure 12 top-right shows the same data as the previous picture showing however the speed-up factor as a function of the number of accelerators. One easily sees that the new heterogeneous version of the code is not only faster than its accelerator-only counterpart but also has a remarkably better behavior from the point of view of hard scaling. This is due to the fact that data moved through MPI communications between different processing nodes is always resident on the host, saving time to move them to and from KNC accelerator. All in all, for massively parallel runs on many accelerators, the heterogeneous code extracts from the same KNC-based hardware system roughly  $2\times$  larger performance than the v1 version.

In Figure 12 bottom-left we show the performance of our code running on the K80 partition. In this case, due to the larger difference in performance between the host-CPU and the accelerator we have a different behavior. Version v2 is faster than version v1, but the gain is less compared to KNC because the gap in performance between the K80 GPU and the host CPU is larger. Scalability, see Figure 12 bottom-right, is good as version v1 because in

both implementations MPI communications are fully overlapped with computation ([34]).

## 8 Analysis of results and conclusions

In this section we analyze our results and outline our conclusions.

The first important contribution of this work highlights the critical role played by data layouts in the development of a common LB code that runs concurrently on CPUs and accelerators and is also *performance*-portable onto different accelerator architectures. The crucial finding in this respect is that data memory organization should support at the same time efficient memory accesses and vector processing. This challenge is made more difficult because different kernels (in our case the critical `propagate` and `collide` routines) have conflicting requirements. Table 2 substantiates the relevance of this problem and quantifies the improvements that we have achieved. Previously used data structures are the AoS layout supporting data-locality, and the *SoA layout* already known to exploit more vectorization especially for GPUs. The problem with these two layouts is that the former allows better performances for Intel architectures but is dramatically bad for GPUs, with performance losses that are up to  $10X$  for `propagate` and  $2X - 5X$  for `collide`. The latter scheme is very efficient on GPUs but it fails on CPUs, as it limits code vectorization and causes memory management overheads (like TLB and cache misses).

This paper introduces two slightly more complex data layouts, the CSoA and the CAoSoA to exploit vectorization on both classes of architecture and still guaranteeing efficient data memory accesses and vector processing for both critical kernels. These data-structures differ from those used in [23] and [25] in the way populations are packed into SIMD vectors; this allows to properly translate operations involved in the `propagate` kernel into SIMD instructions, and to perform aligned memory accesses.

The CSoA layout improves performance on Intel architectures by factors  $2X$  over the AoS for `propagate`

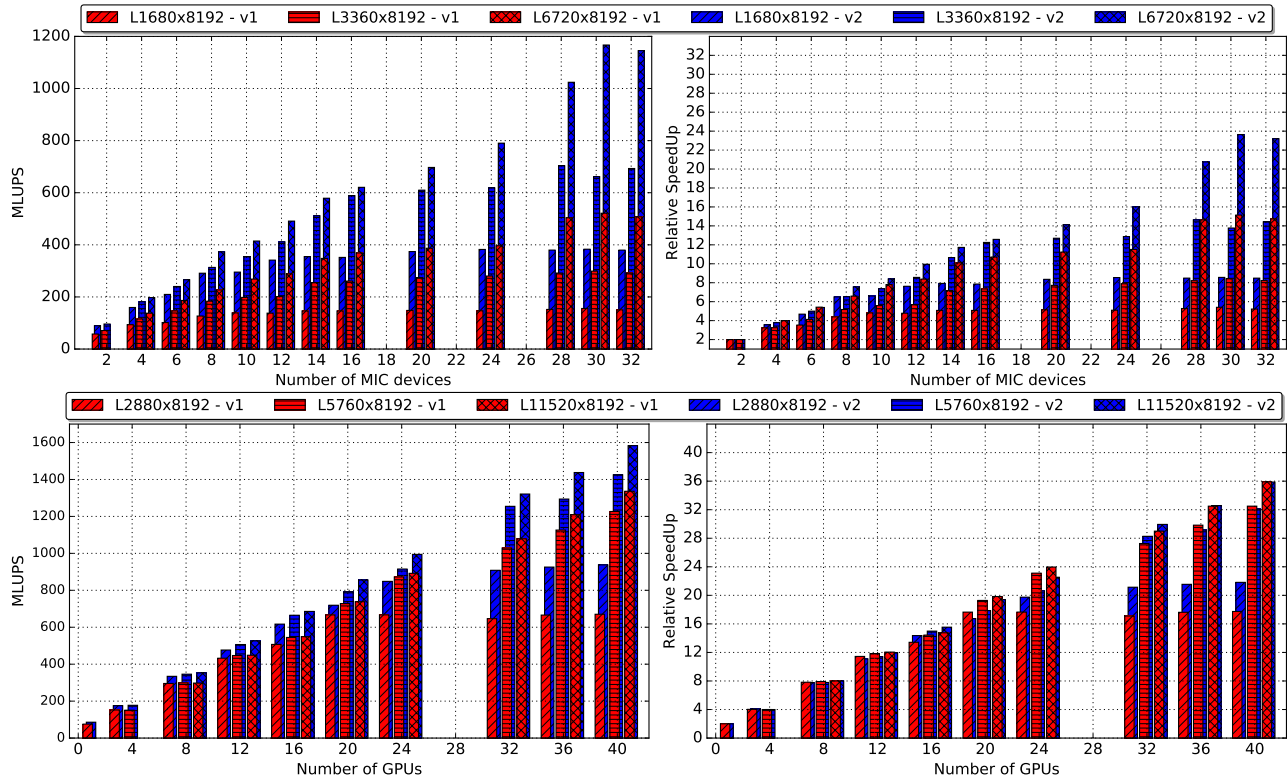


**Figure 12.** Multi-node scalability results measured on the KNC (top) and K80 (down) partitions of the Galileo cluster. We compare performances – MLUPS and relative speedup – on three different lattice sizes of the heterogeneous code described in this paper (v2) with an earlier version (v1) with all critical computational kernels running on accelerators only.

and 1.5X for collide. On GPUs it has also a marginal improvements compared to the already very good results that GPUs have with the original SoA layout. A final improvements is given by the CAoSoA layout, that further increases data locality without introducing vectorization penalties. Again, performance remains substantially stable on GPUs in this case, while there is still a further improvements on Intel architectures for collide ( $\approx 10 - 20\%$ ) and a corresponding penalty for propagate; since the former routine has a bigger impact on overall performance, the CAoSoA layout is the most efficient to be used for the whole code.

The definition of the appropriate layouts has allowed to code our LB application in a common program that executes concurrently on host CPUs and all kinds of accelerators, obviously improving the portability and long-term support of this code.

Another important contribution of this paper is the development of an analytic model (see

section 6.1) able to predict the optimal partitioning of the workload among host-CPU and accelerators; using this model we can automatically tune this parameter for best performance on running systems, or predict performances for not yet available hardware configurations (see section 6.3).

The final result of this contribution is that single node performances can be improved by  $\approx 10 - 20\%$  w.r.t. earlier implementations that simply wasted the computational power offered by the host CPU. Our implementation also significantly improves the (hard)-scaling behavior on relatively large clusters, see Figure 12. This follows from the fact that node-to-node communications in our code do not imply host-accelerator transfers. This improvement is very large on KNC-accelerated clusters, while on GPUs, due to the larger performance unbalance between host and accelerator, the observed improvement is smaller.

In conclusion, an important result of this work is that it is possible to design and implement directive-based codes that are performance-portable across different present – and hopefully future – architectures. This requires an appropriate choice of the data layout, able to meet conflicting requirements of different parts of the code and to match hardware features of different architectures. Defining these data layout is today in the hands of programmers, and still out of the scope of currently available and stable compilers commonly used in the HPC context. For this reason, on a longer time horizon, we look forward to further progress in compilers allowing data definitions that abstract from the actual in-memory implementation, and of tools able to make appropriate allocation choices for specific target architectures.

### Acknowledgements

This work was done in the framework of the COKA, COSA and Suma projects of INFN. We thank CINECA (Bologna, Italy) for access to the Galileo computing cluster. AG has been supported by the European Union's Horizon 2020 research and innovation programme under the Marie Skłodowska-Curie grant agreement No 642069.

### References

- [1] TOP500. Top500 the list, 2016. URL <http://top500.org>. Last visited on 2016-09-01.
- [2] Han T and Abdelrahman T. hiCUDA: High-Level GPGPU Programming. *Parallel and Distributed Systems, IEEE Transactions on* 2011; 22(1): 78–90. DOI:10.1109/TPDS.2010.62.
- [3] Lee S and Eigenmann R. OpenMPC: Extended OpenMP Programming and Tuning for GPUs. In *Proceedings of the 2010 ACM/IEEE International Conference for High Performance Computing, Networking, Storage and Analysis*. SC '10, Washington, DC, USA: IEEE Computer Society. ISBN 978-1-4244-7559-9, pp. 1–11. DOI:10.1109/SC.2010.36.
- [4] Ayguadé E, Badia RM, Bellens P et al. Extending OpenMP to Survive the Heterogeneous Multi-Core Era. *International Journal of Parallel Programming* 2010; 38(5-6): 440–459. DOI:10.1007/s10766-010-0135-4.
- [5] OpenMP. The openmp api specification for parallel programming, 2016. URL <http://www.openmp.org/>. Last visited on 2016-09-01.
- [6] OpenACC. Openacc directives for accelerators, 2016. URL <http://www.openacc-standard.org>. Last visited on 2016-09-01.
- [7] OpenMP. Openmp application program interface version 4.0, 2016. URL <http://www.openmp.org/mp-documents/OpenMP4.0.0.pdf>. Last visited on 2016-09-01.
- [8] NVIDIA. Tesla K80 GPU Accelerator - Board Specification. Technical report, 2015.
- [9] AMD. AMD FirePro W9100 Workstation Graphics. Technical report, 2016.
- [10] George Chrysos IC. Intel Xeon Phi X100 Family Coprocessor - the Architecture. Technical report, 2012.
- [11] Pohl T, Deserno F, Thurey N et al. Performance Evaluation of Parallel Large-Scale Lattice Boltzmann Applications on Three Supercomputing Architectures. In *Proceedings of the 2004 ACM/IEEE Conference on Supercomputing*. SC '04, Washington, DC, USA: IEEE Computer Society. ISBN 0-7695-2153-3, pp. 21–. DOI: 10.1109/SC.2004.37.
- [12] Belletti F, Biferale L, Mantovani F et al. Multiphase lattice boltzmann on the cell broadband engine. *Nuovo Cimento della Societa Italiana di Fisica C* 2009; 32(2): 53–56. DOI:10.1393/ncc/i2009-10379-6.
- [13] Biferale L, Mantovani F, Pivanti M et al. Lattice Boltzmann fluid-dynamics on the QPACE supercomputer. *Procedia Computer Science* 2010; 1(1): 1075–1082. DOI:10.1016/j.procs.2010.04.119. ICCS 2010.
- [14] Pivanti M, Mantovani F, Schifano SF et al. An optimized lattice boltzmann code for BlueGene/Q. In Wyrzykowski R, Dongarra J, Karczewski K et al. (eds.) *Parallel Processing and Applied Mathematics: 10th International Conference, PPAM 2013, Warsaw, Poland, September 8-11, 2013, Revised Selected Papers, Part II*. Lecture Notes in Computer Science, Berlin, Heidelberg: Springer Berlin Heidelberg. ISBN 978-3-642-55195-6, 2014. pp. 385–394. DOI:10.1007/



- 978-3-642-55195-6\_36.
- [15] Mantovani F, Pivanti M, Schifano SF et al. Performance issues on many-core processors: A D2Q37 lattice boltzmann scheme as a test-case. *Computers & Fluids* 2013; 88: 743 – 752. DOI:10.1016/j.compfluid.2013.05.014.
- [16] Bailey P, Myre J, Walsh SD et al. Accelerating lattice Boltzmann fluid flow simulations using graphics processors. In *Parallel Processing, 2009. ICPP'09. International Conference on*. IEEE, pp. 550–557. DOI: 10.1109/ICPP.2009.38.
- [17] Biferale L, Mantovani F, Pivanti M et al. An optimized D2Q37 lattice boltzmann code on GP-GPUs. *Computers & Fluids* 2013; 80: 55 – 62. DOI: 10.1016/j.compfluid.2012.06.003.
- [18] Calore E, Gabbana A, Kraus J et al. Massively parallel latticeboltzmann codes on large GPU clusters. *Parallel Computing* 2016; 58: 1 – 24. DOI:10.1016/j.parco.2016.08.005.
- [19] Crimi G, Mantovani F, Pivanti M et al. Early Experience on Porting and Running a Lattice Boltzmann Code on the Xeon-phi Co-Processor. *Procedia Computer Science* 2013; 18: 551–560. DOI: 10.1016/j.procs.2013.05.219.
- [20] Sano K, Pell O, Luk W et al. FPGA-based Streaming Computation for Lattice Boltzmann Method. In *Field-Programmable Technology, 2007. ICFPT 2007. International Conference on*. pp. 233–236. DOI:10.1109/FPT.2007.4439254.
- [21] Wittmann M, Zeiser T, Hager G et al. Comparison of different propagation steps for the lattice boltzmann method. *CoRR* 2011; abs/1111.0922.
- [22] Shet AG, Sorathiya SH, Krithivasan S et al. Data structure and movement for lattice-based simulations. *Phys Rev E* 2013; 88: 013314. DOI:10.1103/PhysRevE.88.013314.
- [23] Shet AG, Siddharth K, Sorathiya SH et al. On vectorization for lattice based simulations. *International Journal of Modern Physics C* 2013; 24. DOI:10.1142/S0129183113400111.
- [24] Calore E, Demo N, Schifano SF et al. Experience on vectorizing lattice boltzmann kernels for multi- and many-core architectures. In Wyrzykowski R, Deelman E, Dongarra J et al. (eds.) *Parallel Processing and Applied Mathematics: 11th International Conference, PPAM 2015, Krakow, Poland, September 6-9, 2015. Revised Selected Papers, Part I*. Lecture Notes in Computer Science, Cham: Springer International Publishing. ISBN 978-3-319-32149-3, 2016. pp. 53–62. DOI:10.1007/978-3-319-32149-3\_6.
- [25] Valero-Lara P, Igual FD, Prieto-Matas M et al. Accelerating fluidsolid simulations (lattice-boltzmann & immersed-boundary) on heterogeneous architectures. *Journal of Computational Science* 2015; 10: 249 – 261. DOI:10.1016/j.jocs.2015.07.002.
- [26] Valero-Lara P and Jansson J. Heterogeneous cpu+gpu approaches for mesh refinement over lattice-boltzmann simulations. *Concurrency and Computation: Practice and Experience* 2016; : 1 – 20DOI:10.1002/cpe.3919.
- [27] Succi S. *The Lattice-Boltzmann Equation*. Oxford university press, Oxford, 2001.
- [28] Sbragaglia M, Benzi R, Biferale L et al. Lattice Boltzmann method with self-consistent thermo-hydrodynamic equilibria. *Journal of Fluid Mechanics* 2009; 628: 299–309. DOI: 10.1017/S002211200900665X.
- [29] Scagliarini A, Biferale L, Sbragaglia M et al. Lattice Boltzmann methods for thermal flows: Continuum limit and applications to compressible Rayleigh–Taylor systems. *Physics of Fluids (1994–present)* 2010; 22(5): 055101. DOI:10.1063/1.3392774.
- [30] Biferale L, Mantovani F, Sbragaglia M et al. Second-order closure in stratified turbulence: Simulations and modeling of bulk and entrainment regions. *Physical Review E* 2011; 84(1): 016305. DOI:10.1103/PhysRevE.84.016305.
- [31] Biferale L, Mantovani F, Sbragaglia M et al. Reactive Rayleigh-Taylor systems: Front propagation and non-stationarity. *EPL* 2011; 94(5): 54004. DOI:10.1209/0295-5075/94/54004.
- [32] Kraus J, Pivanti M, Schifano SF et al. Benchmarking GPUs with a parallel Lattice-Boltzmann code. In *Computer Architecture and High Performance Computing (SBAC-PAD), 25th International Symposium*

- on. IEEE, pp. 160–167. DOI:10.1109/SBAC-PAD.2013.37.
- [33] Calore E, Gabbana A, Kraus J et al. Performance and portability of accelerated lattice boltzmann applications with openacc. *Concurrency and Computation: Practice and Experience* 2016; 28(12): 3485–3502. DOI:10.1002/cpe.3862.
- [34] Calore E, Marchi D, Schifano SF et al. Optimizing communications in multi-gpu lattice boltzmann simulations. In *High Performance Computing Simulation (HPCS), 2015 International Conference on*. pp. 55–62. DOI:10.1109/HPCSim.2015.7237021.